Molecular and Cellular Biology

Drosophila MCRS2 Associates with RNA Polymerase II Complexes To Regulate Transcription

Ditte Skovaa Andersen, Sunil Jayaramaiah Raja, Julien Colombani, Rachael Louise Shaw, Paul Francis Langton, Asifa Akhtar and Nicolas Tapon

Mol. Cell. Biol. **2010, 30(19):4744. DOI: 10.1128/MCB.01586-09.**
Published Ahead of Print 2 August 2010.

MOLECULAR AND CELLULAR BIOLOGY, Oct. 2010, p. 4744–4755 Vol. 30, No. 19
0270-7306/10/$12.00 doi:10.1128/MCB.01586-09

Drosophila MCRS2 Associates with RNA Polymerase II Complexes To Regulate Transcription▽

Ditte Skovaa Andersen,[1,2] Sunil Jayaramaiah Raja,[3,4] Julien Colombani,[1,2] Rachael Louise Shaw,[1] Paul Francis Langton,[1,5] Asifa Akhtar,[3,4] and Nicolas Tapon[1]*

Apoptosis and Proliferation Control Laboratory, Cancer Research UK, London Research Institute, 44 Lincoln's Inn Fields, London WC2A 3PX, United Kingdom[1]; Institute for Signaling, Developmental Biology and Cancer, Centre National de la Recherche Scientifique Unité Mixte de Recherche 6543, Parc Valrose, 06108 Nice Cedex 2, France[2]; Genome Biology, Gene Expression Unit, European Molecular Biology Laboratory, Meyerhofstrasse 1, 69117 Heidelberg, Germany[3]; Max-Planck-Institut für Immunbiologie, Stübeweg 51, 79108 Freiburg im Breisgau, Germany[4]; and MRC National Institute for Medical Research, Mill Hill, London NW7 1AA, United Kingdom[5]

Received 10 December 2009/Returned for modification 15 January 2010/Accepted 20 July 2010

Drosophila **MCRS2 (dMCRS2; MCRS2/MSP58 and its splice variant MCRS1/p78 in humans) belongs to a family of forkhead-associated (FHA) domain proteins. Whereas human MCRS2 proteins have been associated with a variety of cellular processes, including RNA polymerase I transcription and cell cycle progression, dMCRS2 has been largely uncharacterized. Recent data show that MCRS2 is purified as part of a complex containing the histone acetyltransferase MOF (males absent on first) in both humans and flies. MOF mediates H4K16 acetylation and regulates the expression of a large number of genes, suggesting that MCRS2 could also have a function in transcription regulation. Here, we show that dMCRS2 copurifies with RNA polymerase II (RNAP II) complexes and localizes to the 5′ ends of genes. Moreover, dMCRS2 is required for optimal recruitment of RNAP II to the promoter regions of *cyclin* genes. In agreement with this, dMCRS2 is required for normal levels of *cyclin* gene expression. We propose a model whereby dMCRS2 promotes gene transcription by facilitating the recruitment of RNAP II preinitiation complexes (PICs) to the promoter regions of target genes.**

The initiation of mRNA transcription involves the assembly of a transcription preinitiation complex (PIC), which as a minimum includes RNA polymerase II (RNAP II), Mediator, and six general transcription factors (TFIIA, -B, -D, -E, -F, and -H) at the core promoter DNA region (23, 32, 38). PIC assembly is initiated by the binding of the TATA box binding protein (TBP) subunit of TFIID to the promoter, which is stabilized in the presence of TFIIA and Mediator. Subsequently, TFIIB binds to and stabilizes the TFIIA-TFIIB-Mediator-DNA complex and functions as an adaptor that recruits the preformed RNAP II-TFIIF complex to the promoter. TFIIE and TFIIH then join to form the complete PIC.

Once the PIC has been assembled on the promoter, transcription initiation occurs in several steps, which involve extensive phosphorylation of the C-terminal domain (CTD) of RNAP II (9). Early on in the transition from preinitiation to elongation, phosphorylation of Ser5s in the CTD heptapeptide repeats takes place, and this depends on the activity of the TFIIH-associated kinase cyclin-dependent kinase 7 (Cdk7; mammals)/Kin28 (yeast) (20, 42). Subsequently, Ser2s are phosphorylated by the elongation phase kinase Cdk9 (mammals)/CTDK-1 (yeast) to generate elongation-proficient RNAP II complexes (22, 28). Another Cdk, Cdk8, can negatively regulate RNAP II transcription, partially via its inhibitory effect on Cdk7 activity (3). More recently, it has been suggested that Cdk11^{p110} regulates RNAP II transcription in humans. Thus, Cdk11^{p110} binds to hypo- and hyperphosphorylated RNAP II (47, 52), and antibody-mediated repression of Cdk11^{p110} activity results in inhibition of RNAP II transcription (47).

In addition to the phosphorylation events that control RNAP II activity, modification of the chromatin structure represents an important mechanism for regulating gene expression (41). When the chromatin is in its repressed state, the DNA is wrapped tightly around the histones, creating a barrier to the assembly of the RNAP II PIC at the promoter region. Activation of gene expression is associated with a number of histone modifications that loosen the chromatin structure, including acetylation, methylation, ubiquitylation, and phosphorylation (reviewed in reference 41). Histone H3 and H4 acetylations are particularly frequent toward the 5′ ends of actively transcribed genes and presumably facilitate the initial assembly of the PICs at the promoter region. MOF (males absent on first) is a histone H4 lysine 16 (H4K16)-specific histone acetyltransferase (HAT) in both mammals and *Drosophila* (2, 15, 30, 45, 46). MOF is part of several complexes, including the *Drosophila* male-specific lethal (MSL) complex, which is required for X chromosome dosage compensation (2, 15, 30, 45), the mammalian counterpart of the MSL complex (46), and the MOF-MSL1v1 complex, which mediates p53 acetylation at K120 (11, 25). In addition, MOF copurifies with a number of

* Corresponding author. Mailing address: Apoptosis and Proliferation Control Laboratory, Cancer Research UK, London Research Institute, 44 Lincoln's Inn Fields, London WC2A 3PX, United Kingdom. Phone: 44(0)2072693635. Fax: 44(0)2072693094. E-mail: nicolas.tapon@cancer.org.uk.

▽ Published ahead of print on 2 August 2010.

other proteins, such as the forkhead-associated (FHA) domain-containing protein MCRS2, NSL1-3 (for nonspecific lethal 1 to 3), and MBD-R2, as part of the NSL complex (8, 30, 34, 35).

In the present study, we focus on the function of *Drosophila* MCRS2 (dMCRS2), the *Drosophila* ortholog of human MCRS2 (also known as MSP58). Whereas human MCRS1 and -2 proteins have been associated with a variety of cellular processes, including RNA polymerase I transcription (43) and cell cycle progression (16), dMCRS2 is largely uncharacterized. In addition to the recent observation that human and *Drosophila* MCRS2s form complexes with MOF (8, 34, 30, 35), several other reports suggest that MCRS1 and -2 proteins could function in transcription regulation via interactions with the transcriptional repressor Daxx (27) or the basic region leucine zipper factor Nrf1 (50).

We show that dMCRS2 can be affinity purified in complex with several RNAP II components. Moreover, dMCRS2 associates with RNAP II *in vitro* and colocalizes with RNAP II complexes on polytene chromosomes *in vivo*. Finally, dMCRS2 is required for optimal recruitment of RNAP II to the promoter regions of *cyclin* genes and normal levels of *cyclin A*, *-B*, and *-E* expression. Our findings are consistent with the idea that dMCRS2 is required to promote RNAP II transcription of target genes.

MATERIALS AND METHODS

Cell culture. *Drosophila* S2 cells were grown in Schneider's medium (Invitrogen) supplemented with 10% heat-inactivated fetal bovine serum (Sigma), 50 U/ml penicillin, and 50 μg/ml streptomycin (Invitrogen) at 25°C. Transfections were done using Effectene reagent (Qiagen).

Antibodies. The guinea pig anti-dMCRS2 and rabbit anti-Cdk11 (rabbit 953) antibodies against peptides corresponding to amino acids (aa) 119 to 133 of dMCRS2 and 884 to 898 of Cdk11 were generated and affinity purified by Eurogentec SA (Seraing, Belgium). The rat anti-Cdk11 (385-10) antibody against glutathione *S*-transferase (GST) fused to amino acids 1 to 550 of Cdk11 was generated and affinity purified by Eurogentec SA (Seraing, Belgium). The rabbit anti-dMCRS2 and anti-MOF antibodies were raised against full-length proteins (30, 35). The mouse anti-Rpb1 (7G5) and rabbit anti-TFIIB antibodies were kind gifts from Lazlo Tora (21). The goat anti-RNAP II serum was a kind gift from Arno Greenleaf. The Rpb3 antibody was a kind gift from John Lis (1). The anti-Ser2P RNAP II antibody was purchased from Abcam (chromatin immunoprecipitation [ChIP] grade; ab5095).

Plasmids. dMCRS2, dMCRS2Δ, and Cdk11 coding sequences were PCR amplified and cloned into the pENTR/D-TOPO vector using the following gene-specific primers: for dMCRS2, sense primer CACCATGGAGGCATCAAGAA TAACCG and antisense primer GTTGAGGGGATTCGATGTCTTG; for dMCRS2ΔFHA, sense primer CACCATGGAGGCATCAAGAATAACCG and antisense primer CGGCCACACAAGCAGGCCAG; for Cdk11, sense primer CACCATGGTCAATTCGTCTGGCAGC and antisense primer TCAGAACTT CAGACTGAATCC. To generate dMCRS2, dMCRS2-Flag, dMCRS2ΔFHA-Flag, and hemagglutinin (HA)-Cdk11, dMCRS2, dMCRS2ΔFHA, and Cdk11 coding sequences were cloned into the Gateway pAHW vector (Drosophila Gateway Vector Collection). These included pActin-3×HA and pActin-3×Flag for expression of tagged proteins in S2 cells and pUASp for generation of *UAS-dmcrs2* transgenic lines.

Transgenic flies. To generate the *UAS-dmcrs2* transgenic line, the *pUAS-dmcrs2* construct was introduced into the germ line by injections in the presence of transposase as previously described (7, 39). The *dmcrs2* (5123) and *cdk11* (10516) RNA interference (RNAi) lines were obtained from the Vienna Drosophila RNAi Center (VDRC).

Genotypes. Genotypes were as follows: w^{iso} (see Fig. 1C to C″ and 4A to C″), *hs-FLP; UAS-RNAi-cdk11/Act > cd2 > Gal4, UAS-GFP; hs-FLP; FRT80B, Ubi-GFP, dmcrs2*^{c07041}*/FRT80B, M(3)67c4* (see Fig. 1B to B″), *dmcrs2*^{rG166}*/+* (see Fig. 5A), and *dmcrs2*^{rG166}*/dmcrs2*^{rG166} (see Fig. 5A).

Immunohistochemistry. Mosaic tissues were obtained using the hs-Flp/FLP recombination target (FRT) system (51). Salivary glands, the fat body, and eye imaginal discs were dissected from L3 larvae (120 h after egg laying [AEL]) in 1× phosphate-buffered saline (PBS). Tissues were fixed in 4% formaldehyde in PBS for 20 min at room temperature, washed four times in PBS containing 0.1% Triton X-100 (PBS-T), blocked for 2 h in PBS-T containing 10% goat serum (PBS-TG), and incubated with primary antibodies in PBS-TG overnight at 4°C. Guinea pig anti-dMCRS2 and rat anti-Cdk11 were used at a dilution of 1/500. The next day, cells and tissues were washed, blocked in PBS-TG, and incubated with secondary antibodies at 1/500 dilution (Rhodamine Red-X-conjugated donkey anti-rat and anti-guinea pig antibodies and fluorescein isothiocyanate [FITC]-conjugated donkey anti-rat antibodies from Jackson ImmunoResearch) for 2 h at room temperature. Hoechst (Sigma) was added to the secondary antibody mixture during the last 30 min of the incubation to stain DNA (see Fig. 1C′ and C″). After washes, tissues were mounted in Vectashield. Fluorescence images were acquired using a Zeiss LSM510 confocal laser scanning microscope (25× and 40× objectives) and processed using Adobe Photoshop CS2.

To generate polytene chromosome spreads, salivary glands from female larvae were dissected from L3 larvae (120 h AEL) in 1× PBS and fixed for 10 min in a drop of fix (3.7% paraformaldehyde and 50% acetic acid) on a siliconized slide. The salivary glands were then transferred to a poly-L-lysine-treated slide and overlaid with a coverslip, and the salivary gland cells were broken up by tapping and squeezing the coverslip. Next, the slides were frozen in liquid nitrogen, and the coverslips were removed using a razor blade. Subsequently, slides were washed in 1× PBS and the polytene chromosome preparations were permeabilized in PBS containing 1% Triton X-100 for 10 min, blocked for 2 h in 5% milk in PBS, and incubated with anti-Rpb1 (7G5; 1/100), rabbit anti-MOF (1/100), rabbit anti-TFIIB (1/100), and rabbit and guinea pig anti-dMCRS2 (1/100) antibodies in 5% milk in PBS overnight at 4°C. The next day, slides were washed, blocked in 5% milk in PBS, and incubated with secondary antibodies diluted 1/500 for 2 h at room temperature. After washes, polytene chromosome spreads were mounted in Vectashield. Fluorescence images were acquired using a Zeiss LSM510 confocal laser scanning microscope (40× objective) and processed using Adobe Photoshop CS2.

Tandem affinity purification from S2 cells. Two-step purifications were performed from 1×10^{10} S2 cells expressing recombinant GTC-dMCRS2 or the GTC tag alone as previously described (4) (details on the procedure are available on request). The final eluates from the purifications were resolved by SDS-PAGE on 4 to 12% gradient gels (Invitrogen). Individual protein bands were visualized by Brilliant Blue G colloidal concentrate (Sigma) staining, cut out, and identified by matrix-assisted laser desorption ionization–time of flight (MALDI-TOF) mass spectrometry (MS) at the Taplin Biological Mass Spectrometry Facility.

IP. Immunoprecipitations (IPs) were performed from 1×10^7 (see Fig. 2F and G) or 1×10^8 S2 cells. Cells were lysed in 200 μl (see Fig. 2F and G) or 1 ml buffer B (50 mM Tris-HCl, pH 8, 150 mM NaCl, 0.5% NP-50, 1 mM EGTA, 0.5 M NaF, phosphatase inhibitor cocktail 2 [Sigma], Complete protease inhibitor cocktail [Roche]), and cell extracts were cleared of membranous material by centrifugation at 10,000 rpm for 15 min. For RNase/DNase treatments (see Fig. 3C to G) a modification of buffer B (50 mM Tris-HCl, pH 8, 150 mM NaCl, 5 mM $MgCl_2$, 0.5% NP-50, 0.5 M NaF, phosphatase inhibitor cocktail 2 [Sigma], EDTA-free Complete protease inhibitor cocktail [Roche]) was used to lyse the cells. The cleared extracts were incubated with 250 μg/ml RNase A (Qiagen) and 50 units/ml RNase-free DNase (Roche) for 10 min, and then EDTA was added to a final concentration of 5 mM. For all IPs, extracts were incubated with protein A-Sepharose 4B beads (Amersham) for 1 h to reduce unspecific binding of proteins to the beads in the subsequent purifications. Next, the precleared extracts were incubated with 80 μl of protein A-Sepharose beads and 1 μl of the relevant antibody for 2 h. A rabbit anti-V5 antibody was used in the control purifications. Subsequently, beads were washed 3 times in buffer B, boiled in sample buffer (Invitrogen), and resolved by SDS-PAGE on 4 to 12% Nu-PAGE Bis-Tris gels (Invitrogen).

Western blotting. Proteins were resolved by SDS-PAGE using 4 to 12% gradient gels (Invitrogen) and transferred electrophoretically to polyvinylidene difluoride membranes (Amersham). The membranes were incubated for 1 h in blocking buffer (PBS [137 mM NaCl, 2.7 mM KCl, 4.3 mM Na_2HPO_4, 1.47 mM KH_2PO_4, pH 8], 5% milk) and incubated overnight at 4°C in the same buffer containing primary antibodies at the following dilutions: rabbit anti-dMCRS2, rabbit anti-MOF, rabbit anti-Cdk11, rat anti-Cdk11, rabbit anti-RpS25 (4), rabbit anti-GST (Cell Signaling Technology), and rat anti-HA, 1/1,000; mouse anti-β-tubulin (Developmental Studies Hybridoma Bank) and goat anti-RNAP II serum (kind gift from Arno Greenleaf), 1/2,000; mouse anti-Rpb1 antibody (21), 1/5,000. Membranes were washed three times in PBS-T, blocked for 1 h, and

probed with secondary antibodies diluted 1/5,000 in blocking buffer for 1 h at room temperature. After three washes in PBS-T, chemiluminescence was observed using the ECL-Plus Western blotting detection system (Amersham Biosciences).

Velocity sedimentation. To generate the data shown in Fig. 3B, 5×10^8 S2 cells were treated with 100 μg/ml cycloheximide (Sigma) for 10 min and lysed in 0.6 ml 50 mM HEPES-KOH, pH 7.2, 100 mM KCl, 10 mM $MgCl_2$, 0.1% Triton X-100, 1 mg/ml heparin, 2 mM dithiothreitol (DTT), 100 μg/ml cycloheximide, and RNAguard (Amersham). Cell debris was removed via centrifugation for 10 min at 13,000 rpm, and extracts were resolved on 7.5 to 30% sucrose density gradients by centrifugation for 4.5 h at 39,000 rpm and 4°C using the SW41Ti rotor (Beckman). Finally, 600-μl fractions were collected and stored at −20°C.

dsRNA. Double-stranded RNAs (dsRNAs) were synthesized with a Megascript T7 kit (Ambion). DNA templates for dsRNA synthesis were PCR amplified from fly genomic DNA or plasmids using primers that contained 5′T7 RNA polymerase-binding sites followed by sense or antisense sequences. The primers were designed using the E-RNAi website at the Deutsches Krebsforschungszentrum (DKFZ), Heidelberg, Germany (http://www.dkfz.de/signaling/e-rnai3/).

For Fig. 1E to K′, 3A and B, and 5D, the following primers were used: for *eGFP*, sense primer GGTGGTGCCCATCCTGGT and antisense primer TCG CGCTTCTCGTTGGGG; for *dmcrs2*, sense primer CCGGGGACACCTAGCA CTGTTG and antisense primer GGTGCCAAGCAGATCCTCCTC; and for *cdk11*, sense primer CGCTGAATTTCACATTTCCA and antisense primer GA CGAATTGACCATTTTCGG. The following set of primers was used to generate dsRNA targeting an alternative region of *dmcrs2*: sense primer TCT AGA GAC CAG GAA GGT GAA GCG CAG A and antisense primer GAA TTC CCT CCG AGT TCG ACA ACC AGA CA. For ChIP experiments, the following primers were used: for *T7-dmcrs2* (see Fig. 5C), sense primer 5′-TTA ATA CGA CTC ACT ATA GGG AGA GCG TCT AGA GAC CAG GAA GGT GAA GCG CAG A-3′ and antisense primer 5′-TTA ATA CGA CTC ACT ATA GGG AGA CGC GAA TTC CCT CCG AGT TCG ACA ACC AGA CA-3′; for *dmcrs2*, sense primer 5′-CCG GGG ACA CCT AGC ACT GTT G-3′ and antisense primer 5′-GGT GCC AAG CAG ATC CTC CTC-3′; and for *T7-eGFP*, sense primer 5′-TA ATA CGA CTC ACT ATA GGG AGG ATG GTG AGC AAG G and antisense primer 5′-TA ATA CGA CTC ACT ATA GGG AGG ATC GCG CTT CTC G.

Quantitative real-time PCRs. Total RNA was isolated from wandering third-instar larvae using the RNeasy kit (Qiagen) and treated with RQ1 DNase (Promega). The extracted RNAs (2 μg) were used for first-strand cDNA synthesis with avian myeloblastosis virus (AMV) reverse transcriptase. To measure mRNA levels, quantitative PCRs (qPCRs) were carried out on cDNAs using the following gene-specific primers, which were designed using the PrimerExpress software (see Fig. 3E and 5A and B): for *act*, sense primer (Act3) CAAGTGC GAGTGGTGGAAGTT and antisense primer (Act4) GCAGGTGGTTCCGCT CTTT; for *cycE*, sense primer (CycE1) TGCGGGTAGATAAAGGCATC and antisense primer (CycE2) AATGTGAACAACCGCACTCC; for *cycA*, sense primer (CycA1) GCCAGGTGATCCTTGTGAAT and antisense primer (CycA2) CGACATCTACGACTACTTGTATCAGG; for *cycB*, sense primer (CycE1) TGCGGGTAGATAAAGGCATC and antisense primer (CycE2) AA TGTGAACAACCGCACTCC; for *odsh*, sense primer (Odsh_S_S) CGACAGT TTGGATCACTCGTT and antisense primer (Odsh_R_3) CTGCTGGTGCTC TTCGTCT; for *mbdr-2*, sense primer (MBD-R2_S_2) GAAATACTGGAAGC CAGTGAGG and antisense primer (MBD-R2_R_2) TAGGCCCCCAATGAA AGC; for *cg4479*, sense primer (CG4479_S_1) TAATTGCAAAGGCCGC TAAA and antisense primer (CG4479_R_1) TCACTGGTGGTGACCTTGC; for *dmyc*, sense primer (dMyc_3) GCCGAATGGATGATGGAA and antisense primer (dMyc_4) CCATGTAATTTAATGCCAGTAATACG; for *rp49* (control), sense primer (rp49-1) TCCTACCAGCTTCAAGATGAC and antisense primer (rp49-2) CACGTTGTGCACCAGGAACT. Real-time qPCR was performed with Platinum SYBR green qPCR SuperMix-UDG (Invitrogen) using 2.4 ng of cDNA template and a primer concentration of 300 nM. PCR was carried out in 96-well plates using the real-time qPCR detection system (StepOne Plus; Applied Biosystems). All reactions were performed in three replicates. The relative amount of specific mRNAs for each condition was calculated after normalization to the *rp49* transcript.

RESULTS

dMCRS2 is a nuclear protein required for normal growth and proliferation during development. dMCRS2 belongs to a family of FHA domain proteins, most of which function in transcription regulation, DNA repair, and/or cell cycle progression (13, 17, 24). FHA domains are believed to mediate binding to phosphoserine/phosphothreonine and perhaps phosphotyrosine residues. However, the molecular function of dMCRS2 has not been further studied. To characterize the function of dMCRS2 in more detail, we first analyzed the phenotypic consequences of *dMCRS2* depletion *in vivo*. For this purpose, we obtained three stocks carrying transposon (P-element) insertions in the *dmcrs2* locus ($dmcrs2^{c07041}$, $dmcrs2^{c00114}$, and $dmcrs2^{rG166}$). The *c07041* and *c00114* P elements are inserted at the 5′ end of exon 2 (Fig. 1A) and are predicted to cause deletions of approximately 84% of the dMCRS2 protein. The *l(3)rG166* P element is inserted in the third exon (Fig. 1A) and is predicted to cause a deletion of the last 84 amino acids, including most of the FHA domain. Animals homozygous for $dmcrs2^{rG166}$ die as third-instar larvae but can be rescued to viability by *GAL4/UAS*-driven ubiquitous expression of dMCRS2. Similarly, animals that are transheterozygous for combinations of the $dmcrs2^{c0704}$, $dmcrs2^{c00114}$, and $dmcrs2^{rG166}$ mutations exhibit severe growth defects, and although they survive for an extended period in the third (final) instar, they fail to pupariate. Thus, dMCRS2 is required for proliferation and growth during development.

To analyze the growth defect in more detail, we used the FLP/FRT system (6) to induce mitotic clones of $dmcrs2^{c07041}$ mutant tissue in the eye imaginal discs (the larval precursor of the adult eye) of heterozygous animals. In wild-type animals, only very small $dmcrs2^{c07041}$ mutant clones of a few cells could be recovered (data not shown). The difficulty of obtaining dMCRS2 loss-of-function mutant clones in heterozygous animals might in part be due to their elimination by the surrounding wild-type tissue. In developing *Drosophila* imaginal discs, slow-growing cells are generally eliminated by a process known as cell competition, whereby fast-growing cells actively kill their slower neighbors (18). Minute mutations, which are dominantly acting mutations in ribosomal components, are widely used to alleviate the effects of cell competition (29). By creating mutant clones in a *Minute* background, the proliferation rate of the surrounding tissue is slowed down, allowing unhealthy mutant cells to survive. Thus, green fluorescent protein (GFP)-labeled homozygous $dmcrs2^{c07041}$ mutant clones were generated in eye imaginal discs that are heterozygous for a mutation in a *Minute* gene (Fig. 1B to B″). In this context, large clones of $dmcrs2^{c07041}$ mutant tissue could be recovered (Fig. 1B; mutant cells are labeled by two copies of GFP), showing that $dmcrs2^{c07041}$ mutant clones are indeed eliminated through cell competition by their faster-growing wild-type neighbors. As expected, staining mosaic discs with an anti-dMCRS2 antibody revealed a significant reduction in dMCRS2 protein levels in mitotic clones of $dmcrs2^{c07041}$ mutant tissue (Fig. 1B′). Staining of wild-type salivary glands with our anti-dMCRS2 antibody revealed that the majority of dMCRS2 is in the nucleus (Fig. 1C to C″).

To further investigate the growth/proliferation defect observed in *dmcrs2* mutant animals, we analyzed the effect of dMCRS2 depletion on proliferation and cell cycle progression in cultured *Drosophila* S2 cells. Cells were treated with dsRNA targeting *eGFP* (control) or *dmcrs2* for the indicated number of days, and total cell number was determined (Fig. 1D). Consistent with the growth defect observed *in vivo*, dsRNA-mediated depletion of dMCRS2 slows down and eventually blocks

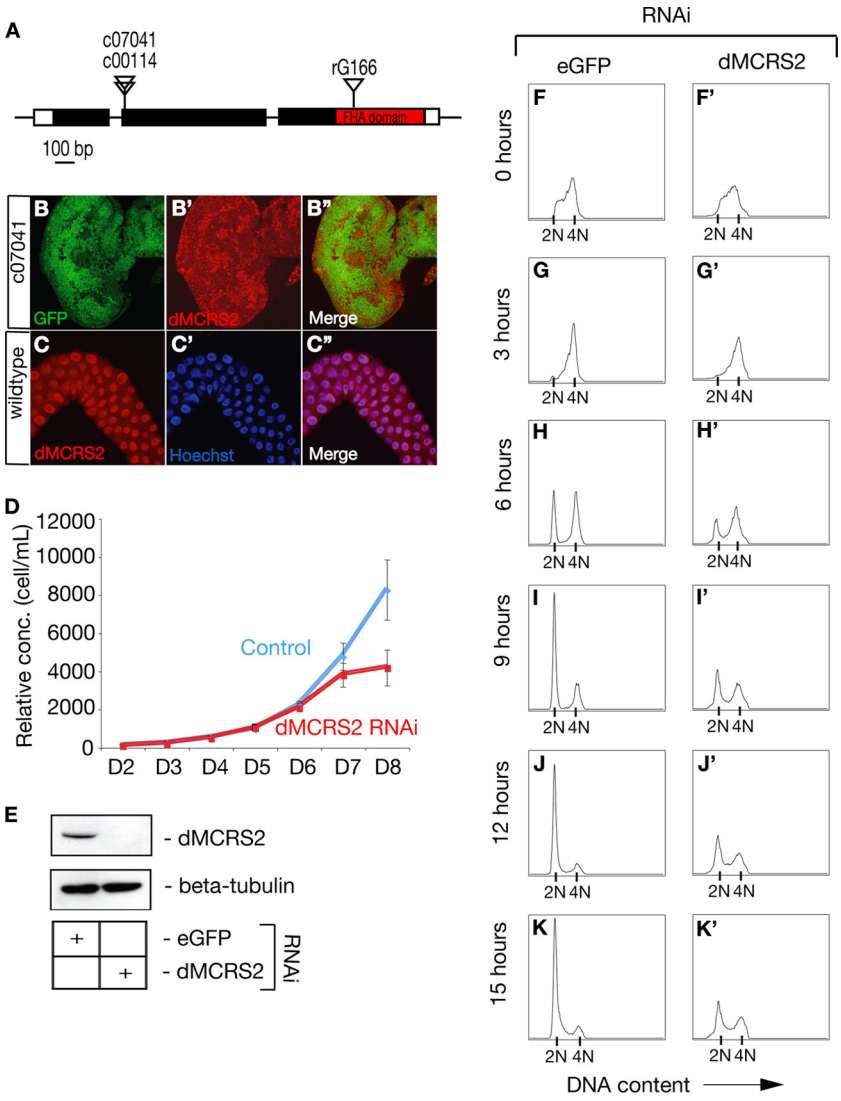

FIG. 1. dMCRS2 is a nuclear protein required for cell and tissue growth. (A) Schematic of the *dmcrs2* locus. The *dmcrs2* locus comprises three exons (black). The 5′ end of the third exon includes a forkhead-associated (FHA) domain (red). The positions of the *c07041*, *c00114*, and *rG166* P elements inserted in *dmcrs2* are indicated. (B to B″) dMCRS2 protein levels are significantly reduced in mitotic clones of $dmcrs2^{c07041}$ mutant tissue. Eye imaginal discs from third-instar larvae are shown. The posterior end is to the left. Mitotic clones of $dmcrs2^{c07041}$ mutant tissue are marked by two copies of GFP (B) and stained with the anti-dMCRS2 antibody in red (B′). (C to C″) dMCRS2 is mainly nuclear. Salivary glands from wild-type third-instar larvae were stained with the anti-dMCRS2 antibody (C) or a nuclear dye (C′). (D) dMCRS2 is required for normal proliferation. Control treated (blue) and dMCRS2-depleted (red) S2 cells were counted once a day from day 2 (D2) to day 7. Error bars represent standard deviations of three independent experiments. (E) Immunoblotting confirms that dMCRS2 protein levels are reduced in cells treated with dsRNA targeting *dmcrs2* after 7 days. Cell extracts prepared from S2 cells treated with dsRNA corresponding to *GFP* (control) or *dmcrs2* for 7 days were immunoblotted for dMCRS2. Anti-β-tubulin was used as a loading control. (F to K′) Depletion of dMCRS2 slows down cell cycle progression. S2 cells were treated with dsRNA targeting GFP (control; F to K) or *dmcrs2* (F′ to K′) for 6 days. Cells were reseeded at a density of 1×10^6 cells/ml and pulse-labeled with BrdU for 15 min. Cells were fixed, stained with propidium iodide, and analyzed by flow cytometry at the indicated time points after the BrdU pulse. The peaks corresponding to the G_1 (2N) and G_2/M (4N) populations are indicated on the *x* axis.

proliferation after about 7 days (Fig. 1D). In accordance with this, dMCRS2 protein levels are significantly reduced after 7 days of dsRNA treatment (Fig. 1E).

To measure the kinetics with which dMCRS2-depleted cells progress through the cell cycle, aliquots of cells treated with dsRNA targeting *eGFP* (control) or *dmcrs2* for 6 days were removed and pulse-labeled with bromodeoxyuridine (BrdU) for 15 min (Fig. 1F to K′). A BrdU pulse can be used to specifically label S-phase cells within an asynchronously growing population of S2 cells. Cells were collected at the indicated time points after the BrdU pulse, and BrdU-positive cells were recorded by flow cytometry. After 6 h, a significant proportion of the control cells have undergone cell division and entered G_1 (Fig. 1H). In contrast, the majority of dMCRS2-depleted cells still remain in S phase and G_2/M (Fig. 1H′). After 12 h nearly all control cells are in G_1, whereas dMCRS2-depleted cells are unsynchronized and present in all phases of the cell cycle (Fig. 1J and J′). Cells depleted of dMCRS2 using an

alternative nonoverlapping dsRNA exhibited a similar abnormal distribution among the different phases of the cell cycle (data available on request), ruling out potential off-target effects. These data show that cells depleted of dMCRS2 proceed through the cell cycle with slower kinetics than control cells, suggesting impaired growth and/or cell cycle progression.

dMCRS2 associates with several RNAP II-associated proteins. We next used a tandem affinity purification method to identify dMCRS2-associated proteins (Fig. 2B). Schneider S2 cells that inducibly express glutathione *S*-transferase (GST)–tobacco etch virus (TEV) protease–calmodulin binding peptide (CBP)-tagged dMCRS2 (GTC-dMCRS2) protein under the control of the metallothionein promoter were generated. GTC-dMCRS2 and GTC alone (control) were purified from approximately 1×10^{10} S2 cells on glutathione-Sepharose beads and cleaved with TEV protease, and then CBP-dMCRS2 and any associated proteins were bound to calmodulin beads, washed, and eluted (Fig. 2B; details of procedures available on request). The final eluates were subjected to SDS-PAGE, and individual protein bands were visualized by Brilliant Blue G colloidal concentrate staining (Fig. 2C). Bands that were present in the dMCRS2 sample but absent in the control sample were carefully excised and subjected to mass spectrometry to identify the proteins (bands marked with numbers in Fig. 2C). In the control sample two faint bands had a migration pattern similar to that of bands in the GTC-dMCRS2 purification (bands marked with asterisks in Fig. 2C, lane 2). To avoid false positives in our GTC-dMCRS2 purification, those contaminants were excised and identified by mass spectrometry.

Interestingly, a number of proteins identified by our mass spectrometry analysis have known or predicted functions in RNAP II transcription (Fig. 2A, red). These include both subunits of the general RNAP II transcription factor TFIIF, the FACT component SSRP (*Drosophila*)/SSRP1 (humans)/Pob3p (yeast), Pitslre (*Drosophila*)/Cdk11^{p110} (humans), CKIIα (*Drosophila*)/CK2α (humans)/Cka2p (yeast), and Psr (*Drosophila*)/JMJD6 (humans). Notably, many of these proteins have previously been reported to copurify with each other and with RNAP II in humans. Thus, Cdk11 has been found to associate with both subunits of TFIIF, CK2, the FACT complex, and hypo- and hyperphosphorylated RNAP II (47), and CK2 has been isolated in complex with TFIIF, Cdk11^{p110}, RNAP II, and SSRP1, all of which it is capable of phosphorylating (14, 26, 33, 48).

The identification of several proteins in our GTC-dMCRS2 purification with known or predicted functions in RNAP II transcription suggests that dMCRS2 is also involved in this process. We did not identify core RNAP II components or the known dMCRS2 partner MOF (30) in our purifications. However, since we performed MS on purified individual bands after SDS-PAGE rather than using a liquid chromatography/MS approach, our characterization of dMCRS2-associated proteins was potentially not exhaustive. Consistent with this idea, we were able to verify the association of endogenous dMCRS2 with MOF (data available on request) and RNAP II (Fig. 3C and D).

dMCRS2 associates with the nuclear RNAP II-associated Pitslre/Cdk11^{p110} protein. We initially sought to verify the association of dMCRS2 with Pitslre (*Drosophila*)/Cdk11^{p110} (humans) (Fig. 2A), which has been found to associate with both the hypo- and hyperphosphorylated forms of RNAP II and is required for RNAP II transcription in human cells (47). The fly Cdk11 protein was originally named after a conserved PITSLRE cyclin-binding motif in its kinase domain (40). Given that Pitslre is the closest fly homologue of Cdk11^{p110}, we refer to the fly protein as Cdk11. We generated an antibody directed against a bacterially expressed Cdk11 fragment (aa 1 to 550). The specificity of the antibody was tested on *cdk11* RNAi-expressing clones in the salivary glands using the Flipout/GAL4 technique (details available on request) (51). Nuclear Cdk11 was significantly reduced in clones expressing the Cdk11 RNAi construct (data available on request). Staining of wild-type imaginal discs (data not shown) or fat body tissue (data available on request) showed that dMCRS2 and Cdk11 are both present in the nucleus but not the nucleolus, consistent with putative functions in RNAP II transcription. To confirm that fly Cdk11, like human Cdk11, is associated with RNAP II, we used a goat anti-*Drosophila* RNAP II serum, which was previously shown to recognize several of the *Drosophila* RNAP II subunits (49), to immunoprecipitate endogenous RNAP II. Immunoblotting of RNAP II and V5 (control) precipitates with our rat anti-Cdk11 antibody showed that a fraction of endogenous fly Cdk11 is indeed associated with RNAP II (Fig. 2D). We next tested the ability of endogenous dMCRS2 to coimmunoprecipitate Cdk11 (Fig. 2E). Immunoblotting of Cdk11, dMCRS2, and control (anti-V5) precipitates with our anti-Cdk11 antibody revealed that endogenous Cdk11 coimmunoprecipitates with dMCRS2 (Fig. 2E). Moreover, this interaction persists after treatment with RNase and DNase, showing that the Cdk11-dMCRS2 interaction, though not necessarily direct, is not bridged by DNA/RNA (data available on request). Finally, we find that Cdk11 is unable to associate with dMCRS2 lacking its C-terminal FHA domain (dMCRS2ΔFHA-Flag) (Fig. 2F and G), suggesting that the FHA domain of dMCRS2 is required for its association with HA-Cdk11.

dMCRS2 associates with RNAP II complexes. To analyze whether dMCRS2, like Cdk11, associates with RNAP II, we first examined the velocity sedimentation profiles of all three proteins on a sucrose gradient (Fig. 3B). To examine the sedimentation profile of endogenous Cdk11, we used a rabbit anti-Cdk11 antibody that recognizes a C-terminal region of Cdk11 (aa 884 to 898). The specificity of the antibody was verified on extracts from cells treated with dsRNA targeting *eGFP* (control) or *Cdk11* for 4 days (Fig. 3A).

Extract from S2 cells was resolved by velocity sedimentation on a 7.5 to 30% sucrose gradient, and fractions were collected and immunoblotted for the presence of dMCRS2, Cdk11, and RNAP II. To detect RNAP II subunits, we used the goat anti-*Drosophila* RNAP II serum, which recognizes several of the *Drosophila* RNAP II subunits (49). For comparison, the 40S ribosomal subunit fractions were marked using an anti-RpS25 antibody. The majority of dMCRS2 protein cosediments with Cdk11 and RNAP II in fractions slightly higher up the gradient than the 40S ribosomal subunit fractions (Fig. 3B). These data suggest that dMCRS2, like Cdk11 (Fig. 2D), might be associated with RNAP II complexes. To analyze this in more detail, RNAP II was immunoprecipitated from S2 cells using the goat anti-*Drosophila* RNAP II serum. Immunoblot

A

ID (Drosophila/Humans/Yeast[1])	Band # (peptides)	Coverage (%)	Predicted function
dMCRS2/p58 (63.5 kDa)	4 (14)	24.7	Chromatin remodelling/RNAP I transcription
Pitslre/Cdk11 (109 kDa)	1 (24)	23.6	Transcription/splicing
TFIIFα/GTF2F1/Rap74 (64.4 kDa)	4 (24)	30.2	Transcription
TFIIFβ/GTFII2F2/Rap30 (32.1 kDa)	9 (19)	51.3	Transcription
SSRP/SSRP1/Pob3p (81.5 kDa)	3 (31)	36.1	Chromatin remodeling/transcription regulation
Psr/JMJD6 (47.0 kDa)	6 (13)	32.6	Chromatin remodeling/transcription regulation
CKIIα/CK2α/Cka2p (40.0 kDa)	8 (18)	54.0	Survival/Transcription
eIF3-S9/eIF3S9/Prt1 (80.4 kDa)	3 (28)	37.8	Translation initiation
Int6/eIF3S6 (51.1 kDa)	7 (14)	32.2	Translation initiation/nonsense mediated decay
Pabp/PABPC1/pabp (69.9 kDa)	5 (17)	34.5	Translation initiation
CBP80/NCBP1/STO1 (93.2 kDa)	2 (13)	22.6	RNA cap binding/nonsense mediated decay
CG8611/DDX31/DBP7 (108 kDa)	1 (17)	20.4	rRNA processing
Pit/DDX18/Has1p (76.9 kDa)	2 (14)	23.8	rRNA processing
B52/Srp55 (39.8 kDa)	6 (18)	28.5	Splicing/Alternative splicing
Hfp/PUF60 (58 kDa)	5 (17)	36.6	Splicing/Alternative splicing
CG7843/ARS2 (107 kDa)	1 (38)	34.0	Unknown
CG4887/RBM10 (114 kDa)	1 (13)	18.5	Unknown
CG6904/GSY1/UDP-glucose-starch glucosyltransferase (79.2 kDa)	4 (20)	34.1	Glycogen synthesis

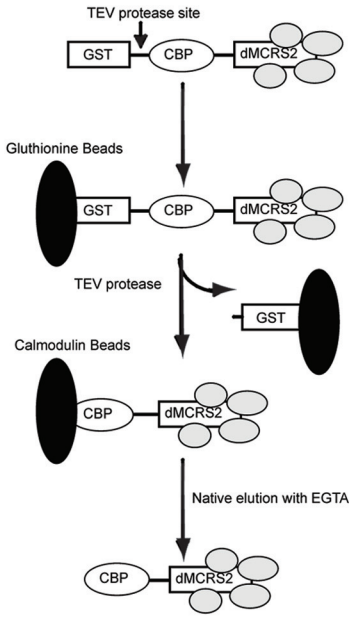

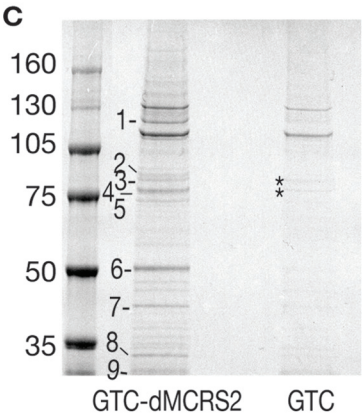

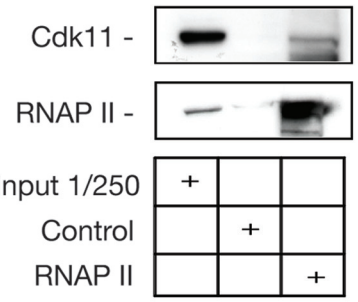

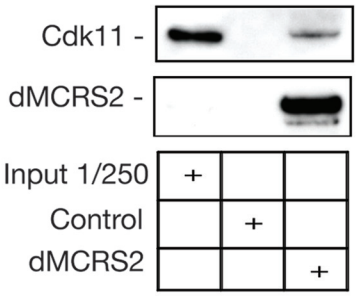

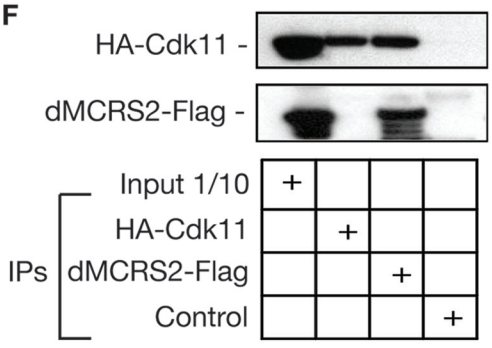

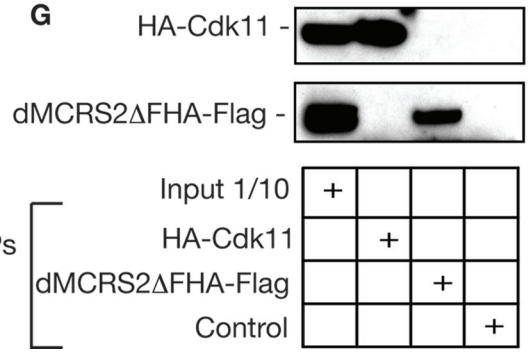

FIG. 2. dMCRS2 associates with Cdk11 and other proteins that function in RNAP II transcription. (A) Table summarizing proteins isolated in complex with GTC-dMCRS2. When a protein does not have an obvious homologue in yeast, the fly and human designations are indicated. The band of origin and the number of unique peptide matches are listed for each of the identified proteins. Proteins that are thought to play a role in RNAP II transcription are highlighted in red. (B) Schematic of the two-step purification procedure used to identify dMCRS2-associated proteins (details of the procedure are available on request). (C) The two-step purifications were performed from S2 cells expressing GTC-dMCRS2 or the GTC tag alone. The final eluates were resolved on a 4 to 12% NuPAGE Bis-Tris gel and stained with Brilliant Blue G colloidal concentrate. Visible bands were excised and identified by MALDI-TOF mass spectrometry. (D to E) Cdk11 associates with dMCRS2 and RNAP II. RNAP II (D), dMCRS2 (E), and control (anti-V5) (D and E) immunoprecipitates were blotted for the presence of Cdk11 using an anti-Cdk11 antibody (top), RNAP II using an anti-Rpb1 antibody (D, bottom) (21), and dMCRS2 using the anti-dMCRS2 antibody (E, bottom). (F and G) Deletion of the dMCRS2 FHA domain abolishes its interaction with Cdk11. dMCRS2-Flag (F), dMCRS2ΔFHA-Flag (G), HA-Cdk11 (F and G), and control (anti-V5) (F and G) immunoprecipitates were blotted for the presence of HA-Cdk11 using an anti-HA antibody (top) and dMCRS2 using the anti-dMCRS2 antibody (bottom).

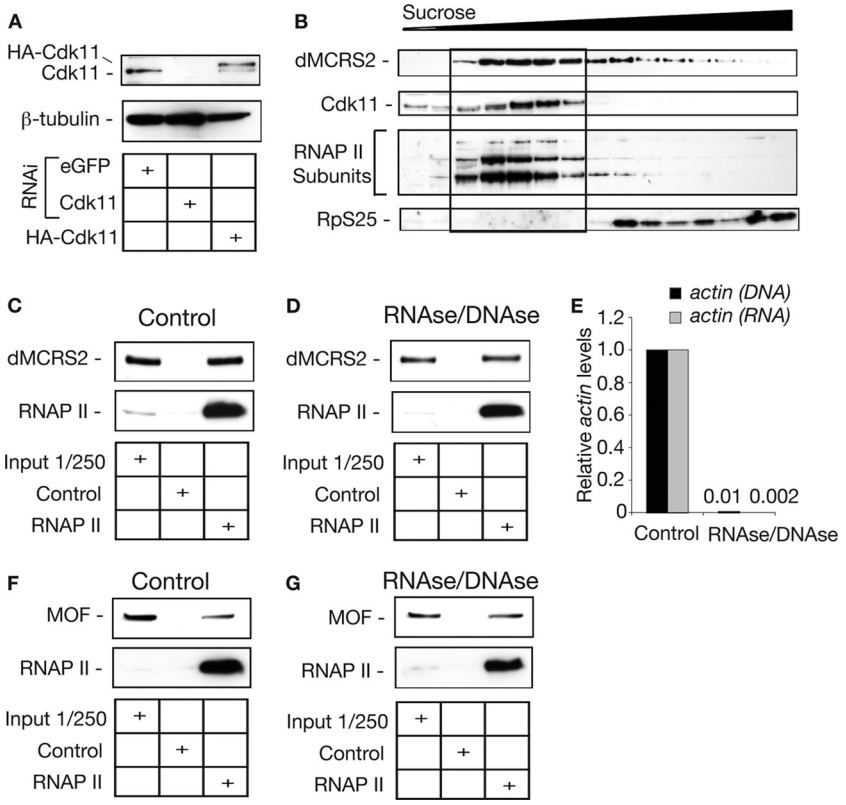

FIG. 3. dMCRS2 associates with RNAP II. (A) The specificity of the anti-Cdk11 antibody was confirmed by immunoblotting on cell extracts prepared from S2 cells treated with dsRNA corresponding to *GFP* (control) or *dmcrs2* for 4 days and from cells expressing HA-Cdk11. Anti-β-tubulin was used as a loading control. (B) dMCRS2 and Cdk11 cosediments with RNAP II on a sucrose gradient. Cell extracts were resolved by velocity sedimentation on a 7.5 to 35% sucrose gradient for 4 h at 39,000 rpm. The presence or absence of dMCRS2, Cdk11, and RNAP II in the different fractions was revealed by Western blotting. The goat anti-*Drosophila* RNAP II serum recognizes several of the *Drosophila* RNAP II subunits, as previously shown (49). Fractions containing the 40S subunit were identified by probing for the small ribosomal protein RpS25. (C, D, F, and G) dMCRS2 and MOF coimmunoprecipitate with RNAP II. RNAP II and control immunoprecipitations were performed using the goat anti-RNAP II serum and an anti-V5 antibody (control) in the presence (D and G) or absence (C and F) of RNase and DNase. RNAP II and control (anti-V5) were blotted for the presence of dMCRS2 using an anti-dMCRS2 antibody (C and D, top), MOF using an anti-MOF antibody (F and G, top), and RNAP II using an anti-Rpb1 antibody (C, D, F, and G, bottom) (21). (E) To verify the efficiency of the RNase/DNase treatments, *act* RNA (see Materials and Methods) and DNA levels were measured by quantitative PCR in control and RNase/DNase-treated samples.

analysis of RNAP II precipitates using an anti-dMCRS2 antibody revealed that endogenous dMCRS2 is associated with RNAP II (Fig. 3C, top; data available on request). In addition, we found that a substantial fraction of the dMCRS2-associated HAT, MOF, coimmunoprecipitates with RNAP II (Fig. 3F, top). Importantly, the dMCRS2-RNAP II and MOF-RNAP II interactions were not sensitive to treatment with RNase and DNase, showing that the interactions of dMCRS2/MOF with RNAP II are not bridged by RNA/DNA (Fig. 3C to G). Using anti-dMCRS2 and anti-MOF antibodies, we were also able to coimmunoprecipitate RNAP II, albeit less efficiently (data available on request). Together, these observations support the idea that dMCRS2, like MOF, plays a role in RNAP II transcription.

dMCRS2 colocalizes with RNAP II preinitiation complexes *in vivo*. To further analyze the association of dMCRS2 with RNAP II complexes, we costained polytene chromosome spreads prepared from the salivary glands of developing third-instar larvae (see Materials and Methods) with anti-dMCRS2 (Fig. 4A) and anti-RNAP II (Fig. 4A′) antibodies as previously described in reference 21. Stainings revealed the localization of dMCRS2 in distinct bands on the polytene chromosomes, many of which colocalized with RNAP II (Fig. 4A to A″). This indicates that dMCRS2 is indeed associated with a subgroup of RNAP II complexes *in vivo*. To characterize this subgroup of RNAP II complexes in more detail, we costained polytene chromosome spreads with anti-dMCRS2 and anti-TFIIB (21) antibodies (Fig. 4B to B″). TFIIB is required for assembly of the RNAP II preinitiation complex but is released prior to or concomitant with the phosphorylation events required for RNAP II elongation (37, 54). Our stainings show that dMCRS2 colocalizes with TFIIB, suggesting that dMCRS2, like TFIIB, may be associated with RNAP II PICs. Consistent with this, dMCRS2 does not colocalize with phosphorylated early (phospho-Ser5) or late (phospho-Ser2) elongating RNAP II complexes (data available on request). Moreover, our costainings reveal an extensive overlap between dMCRS2- and MOF-specific bands (Fig. 4C to C″), in agreement with the existence of a dMCRS2-MOF complex *in vivo*.

dMCRS2 is bound to the promoter-proximal regions of autosomal and X-linked genes. To obtain a high-resolution view of the binding of dMCRS2 on individual genes, chromatin

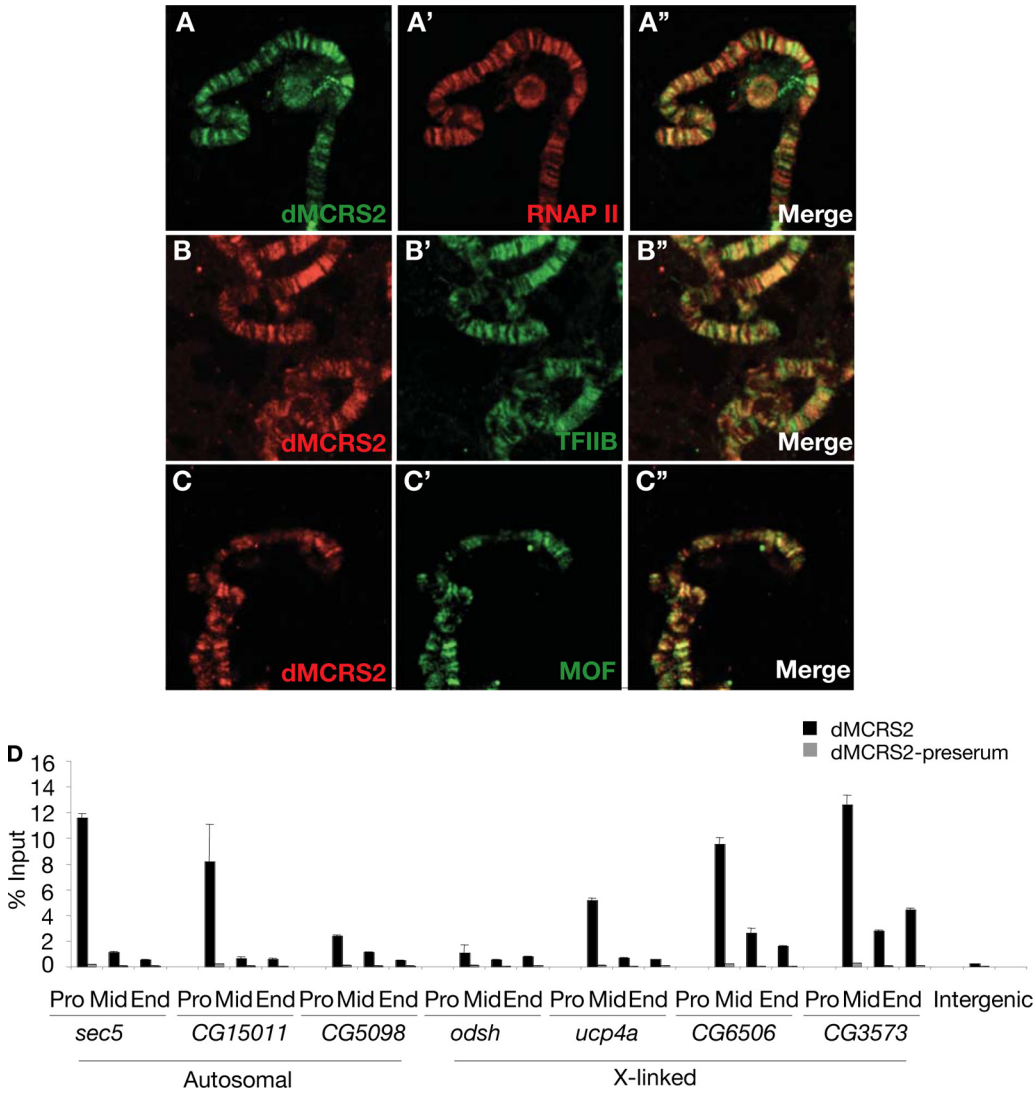

FIG. 4. dMCRS2 colocalizes with a subgroup of RNAP II complexes at the promoter regions of autosomal and X-linked genes. dMCRS2 colocalizes with RNAP II, TFIIB, and MOF on polytene chromosomes. (A to C″) Polytene chromosome spreads were prepared from third-instar female larvae and stained with dMCRS2 (A, B, and C), RNAP II (A′), TFIIB (B′), and MOF (C′). dMCRS2 is bound to the promoter regions of autosomal and X-linked genes. (D) Chromatin immunoprecipitation (ChIP) analyses for S2 cells using preserum (dMCRS2) and the rabbit anti-dMCRS2 antibody. Immunoprecipitated DNA was amplified by real-time PCRs (primer sets are available on request). Four X-linked genes (*odsh*, *ucp4a*, *CG6506*, and *CG3573*) and three autosomal genes (*sec5*, *CG15011*, and *CG5098*) were evaluated using primers positioned at the promoter (Pro), middle (Mid), and end of the transcribed sequence. To confirm the specificity of the binding of each of the antibodies to the tested genes, a primer set amplifying an intergenic region was included (negative control). Percent input is determined as the amount of precipitated DNA relative to input DNA. Error bars represent standard errors of means of four independent experiments.

immunoprecipitation (ChIP) assays were conducted on wild-type S2 cells. Since we have shown that dMCRS2 and MOF colocalize extensively on polytene chromosomes (Fig. 4C to C″), we chose a set of X chromosome and autosomal genes that are known to bind MOF (19). In addition we included a gene, *odsh*, which is neither bound or transcriptionally regulated by MOF (19). Primers designed for the promoter region, middle, and end of the transcribed region were used. Interestingly, we found that, like MOF (19), the majority of dMCRS2 binds to the promoter-proximal regions of these genes (Fig. 4D). As expected, the MOF nontarget gene *odsh* is also not bound by dMCRS2 (Fig. 4D) (19). This is consistent with a role for dMCRS2 in early events of RNAP II transcription.

dMCRS2 is required for RNAP II recruitment to the promoter regions of *cyclin* genes. dMCRS2-depleted cells arrest at multiple stages of the cell cycle, suggesting that dMCRS2-regulated genes might include *cyclin* genes, whose mRNAs are highly unstable and have to be synthesized at each round of division. Furthermore, NSL components were bound to the *cyclinE*, *-A*, and *-B* promoters in a ChIP sequencing (ChIP-seq) experiment (35). To explore the idea that dMCRS2 might be required for *cyclin* expression, we prepared RNA extracts from third-instar *dmcrs2* mutant larvae (Fig. 5A) and analyzed the mRNA levels of different *cyclin* genes by quantitative PCR (qPCR). Removing one copy of *dmcrs2* had no effect on mRNA levels of any of the tested

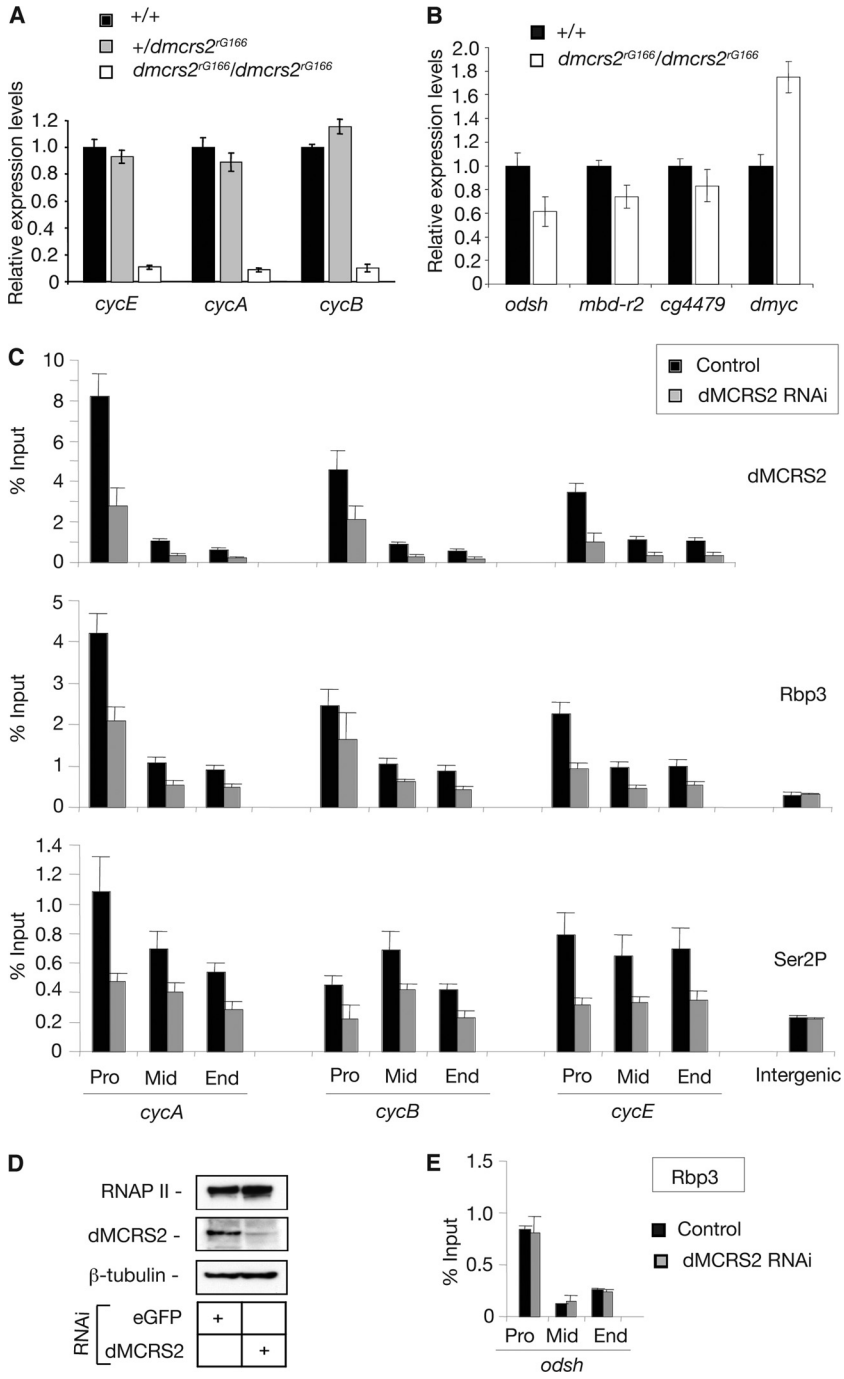

FIG. 5. dMCRS2 is required for RNAP II recruitment to the promoter regions of *cycA*, *cycB*, and *cycE*. (A and B) RNA was extracted from control (+/+), heterozygous (+/*dmcrs2*^{rG166}), and homozygous (*dmcrs2*^{rG166}/*dmcrs2*^{rG166}) *dmcrs2* mutant third-instar larvae. *cycE*, *cycA*, and *cycB* (A) and *odsh*, *mbd-R2*, *cg4479*, and *dmyc* (B) mRNA levels were measured after 1st-strand cDNA synthesis by qPCR (see Materials and Methods). Target mRNA levels were compared between different samples by normalization to levels for the large ribosomal protein transcript (*rpl49*). (C and E) ChIP analyses from enhanced GFP (eGFP) (control)- or dMCRS2-depleted S2 cells using anti-dMCRS2 (C, top), anti-Rpb3 (RNAP II subunit; C, middle, and E), and Ser2P (Ser5 phosphorylated CTD of RNAP II; C, bottom) antibodies. Immunoprecipitated DNA was amplified by real-time PCRs (primer sets are available on request). The *cycA* (C), *cycB* (C), *cycE* (C), and *odsh* (E) genes were evaluated using primers positioned at the promoter (Pro), middle (Mid), and end of the transcribed sequence. To confirm the specificity of the binding of each of the antibodies to the tested genes, a primer set amplifying an intergenic region was included (negative control). Percent input is determined as the amount of precipitated DNA relative to input DNA. Error bars represent standard errors of means of four independent experiments. (D) Total levels of RNAP II are unchanged in cells depleted of dMCRS2. Cell extracts prepared from S2 cells treated with dsRNA corresponding to *GFP* (control) or *dmcrs2* for 7 days were immunoblotted for RNAP II and dMCRS2 using anti-Rpb1 (top) and anti-dMCRS2 (middle) antibodies. Anti-β-tubulin was used as a loading control (bottom). (E) Depletion of dMCRS2 does not affect recruitment of RNAP II to the dMCRS2 nontarget gene *odsh*.

cyclin genes (*dmcrs2*^{rG166}/+) (Fig. 5A). In contrast, *cyclinE*, *cyclinA*, and *cyclinB* levels were reduced by 80 to 90% in homozygous *dmcrs2* mutant larvae (*dmcrs2*^{rG166}/*dmcrs2*^{rG166}) (Fig. 5A). Thus, dMCRS2 is required for normal levels of *cyclinE*, *-A*, and *-B* transcripts *in vivo*. We also analyzed the expression levels of a number of dMCRS2 nontarget genes (35) in control and *dmcrs2* mutant larvae (*dmcrs2*^{rG166}/*dmcrs2*^{rG166}) (Fig. 5B). These genes are not directly bound by dMCRS2, and accordingly we found that their expression levels were only slightly reduced (*odsh*, *mbd-R2*, and *cg4479*) or even upregulated (*dmyc*) (Fig. 5B) in *dmcrs2* mutant animals. The modest changes in the expression levels of these genes might be an indirect effect of reducing dMCRS2 levels, since dMCRS2 is present on the promoters of approximately 55% of active genes (35).

Using ChIPs from control and dMCRS2-depleted cells, we confirmed that RNAi treatment leads to a reduction of dMCRS2 at the promoters of the *cyclin* genes (Fig. 5C, top row). Interestingly, we observe that dMCRS2 depletion leads to reduced levels of the RNAP II subunit Rpb3 and RNAP II phospho-Ser2 on *cyclinA* and *-E* (Fig. 5C, middle and bottom rows). The effect is less clear with *cyclinB*, in accordance with the weaker dMCRS2 loss from that promoter (Fig. 5C, top row). Using an alternative dsRNA to deplete dMCRS2 levels also led to reduced levels of the RNAP II subunit Rpb3 and RNAP II phospho-Ser2 on *cyclin* genes (data available on request), ruling out off-target effects. Importantly, the reduced binding of RNAP II to the promoters of *cyclin* genes is not an indirect consequence of altered RNAP II levels, since the total level of RNAP II in dMCRS2-depleted cells is unchanged (Fig. 5D). Moreover, recruitment of RNAP II to the *odsh* gene, which is not a target of dMCRS2 (Fig. 4D), is unaffected in dMCRS2-depleted cells (Fig. 5E). Together, these results suggest that dMCRS2 is required for loading of RNAP II complexes on the *cyclin* gene promoters.

DISCUSSION

Drosophila MCRS2 and its human homologue, MCRS2, are 59% identical, with the highest level of homology being in the FHA domain. Whereas dMCRS2 is largely uncharacterized, MCRS1 and -2 have been linked with a variety of cellular processes, RNAP I-dependent transcription, transcriptional repression, and cell cycle control, though these functions remain poorly understood (12, 16, 27, 43, 50).

We show here that dMCRS2 is an essential nuclear protein required for cell cycle progression and growth during development (Fig. 1). Our data show that dMCRS2 physically associates with Cdk11 and RNAP II and colocalizes with RNAP II PICs on polytene chromosomes *in vivo* (Fig. 2, 3, and 4). Consistent with this, dMCRS2 is required for optimal binding of RNAP II components to the *cyclin* promoter regions and for normal levels of *cyclin* gene expression (Fig. 5).

Our demonstration of the colocalization of dMCRS2 with RNAP II on numerous sites on polytene chromosomes is in agreement with a recent ChIP-seq analysis, which revealed that dMCRS2 is present on the promoters of over 4,000 genes, correlating with 55% of active genes (35). Furthermore, gene expression profiling studies show that dMCRS2 depletion elicits the downregulation of over 5,000 genes (35). This essential function as a broad-specificity transcriptional regulator is reflected by the extreme growth defect of dMCRS2-depleted cells both *in vivo* and in cell culture (Fig. 1) and in the fact that dMCRS2 has been recovered as a hit in RNAi screens for diverse cellular functions such as centrosome maturation and Hedgehog signaling (10, 31).

In accordance with its pleiotropic function, dMCRS2 can be purified with a number of proteins, from NSL components (8, 34, 30, 35) to members of the RNAP II machinery (this study). Moreover, dMCRS2 colocalizes with RNAP II PICs on polytene chromosomes *in vivo* (Fig. 4A to A″), suggesting that it may regulate an early step in the recruitment and/or assembly of RNAP II PICs. This is consistent with the majority of dMCRS2 binding to the promoter regions of autosomal and X-linked genes (Fig. 4D) (35) and the fact that dMCRS2 is required for the loading of RNAP II components to *cyclin* gene promoters (Fig. 5C). Thus, dMCRS2 appears to be an important transcriptional regulator, and our data represent the first evidence for a physical connection between dMCRS2 and the core transcriptional machinery. While our results suggest that dMCRS2 associates with RNAP II complexes via protein-protein interactions (Fig. 3C to E), future studies will need to establish the exact molecular nature of this connection.

Interestingly, MCRS2 and dMCRS2 copurify with the MOF HAT independently of the dosage compensation MSL complex (11, 30). Furthermore, we observe that dMCRS2 coimmunoprecipitates and colocalizes extensively with MOF on polytene chromosomes (Fig. 4C to C″; data available on request) (35). MOF, as well as binding to the 3′ ends of MSL targets along the male X chromosome, is also found on numerous promoter regions, both on the X chromosome and on autosomes in both sexes (19). Since MCRS2 also binds to promoters, it is possible that dMCRS2 and MOF could function in concert in transcriptional regulation. However, despite the evidence that MOF regulates a broad range of both X-linked and autosomal genes (19), no physical connection between the putative dMCRS2-MOF NSL complex (30) and RNAP II complexes has been established so far. We show here that both dMCRS2 and MOF associate with core RNAP II complexes in cultured cells (Fig. 3C to G).

dMCRS2 may promote transcription by different mechanisms. Through its HAT activity, dMCRS2-associated MOF may create a relaxed chromatin state favorable to PIC assembly, either by inducing the physical weakening of DNA/histone or histone/histone interactions (44) or by promoting the recruitment of bromodomain-containing factors (36). dMCRS2 may also induce PIC formation by recruiting the preformed RNAP II/TFIIF complex and/or promoting transcription elongation through the recruitment of CK2 and the FACT complex, which facilitates transcription elongation by remodeling chromatin (5). However, whether these different dMCRS2-containing complexes regulate common target genes or whether they represent distinct transcriptional regulators remains to be investigated. In summary, we propose a model where dMCRS2 binds to multiple sites along the chromosomes and promotes the recruitment of RNAP II PICs to target genes.

ACKNOWLEDGMENTS

We are grateful to the Bloomington *Drosophila* Stock Center and the Vienna *Drosophila* RNAi Center and H. McNeill for fly stocks, and L. Tora, A. Greenleaf, and the Developmental Studies Hybridoma Bank for antibodies. We thank T. Gilbank, Steve Murray, and Frances Earl for transgenic injections, S. Pinchin for advice on polytene chromosome preparation, the LRI FACS lab for help with FACS analysis, and the Taplin Biological Mass Spectrometry Facility for protein identification. We are grateful to S. Leevers, D. Ish-Horowicz, and C. Hill for critical reading of the manuscript.

This work was funded by Cancer Research UK and the European Molecular Biology Organization.

REFERENCES

1. **Adelman, K., M. T. Marr, J. Werner, A. Saunders, Z. Ni, E. D. Andrulis, and J. T. Lis.** 2005. Efficient release from promoter-proximal stall sites requires transcript cleavage factor TFIIS. Mol. Cell **17:**103–112.
2. **Akhtar, A., and P. B. Becker.** 2000. Activation of transcription through histone H4 acetylation by MOF, an acetyltransferase essential for dosage compensation in Drosophila. Mol. Cell **5:**367–375.
3. **Akoulitchev, S., S. Chuikov, and D. Reinberg.** 2000. TFIIH is negatively regulated by cdk8-containing mediator complexes. Nature **407:**102–106.
4. **Andersen, D. S., and S. J. Leevers.** 2007. The essential Drosophila ATP-binding cassette domain protein, pixie, binds the 40 S ribosome in an ATP-dependent manner and is required for translation initiation. J. Biol. Chem. **282:**14752–14760.
5. **Belotserkovskaya, R., and D. Reinberg.** 2004. Facts about FACT and transcript elongation through chromatin. Curr. Opin. Genet. Dev. **14:**139–146.
6. **Blair, S. S.** 2003. Genetic mosaic techniques for studying Drosophila development. Development **130:**5065–5072.
7. **Brand, A. H., and N. Perrimon.** 1993. Targeted gene expression as a means of altering cell fates and generating dominant phenotypes. Development **118:**401–415.
8. **Cai, Y., J. Jin, S. K. Swanson, M. D. Cole, S. H. Choi, L. Florens, M. P. Washburn, J. W. Conaway, and R. C. Conaway.** 2010. Subunit composition and substrate specificity of a MOF-containing histone acetyltransferase distinct from the male-specific lethal (MSL) complex. J. Biol. Chem. **285:**4268–4272.
9. **Dahmus, M. E.** 1995. Phosphorylation of the C-terminal domain of RNA polymerase II. Biochim. Biophys. Acta **1261:**171–182.
10. **Dobbelaere, J., F. Josue, S. Suijkerbuijk, B. Baum, N. Tapon, and J. Raff.** 2008. A genome-wide RNAi screen to dissect centriole duplication and centrosome maturation in Drosophila. PLoS Biol. **6:**e224.
11. **Dou, Y., T. A. Milne, A. J. Tackett, E. R. Smith, A. Fukuda, J. Wysocka, C. D. Allis, B. T. Chait, J. L. Hess, and R. G. Roeder.** 2005. Physical association and coordinate function of the H3 K4 methyltransferase MLL1 and the H4 K16 acetyltransferase MOF. Cell **121:**873–885.
12. **Du, X., Q. Wang, Y. Hirohashi, and M. I. Greene.** 2006. DIPA, which can localize to the centrosome, associates with p78/MCRS1/MSP58 and acts as a repressor of gene transcription. Exp. Mol. Pathol. **81:**184–190.
13. **Durocher, D., J. Henckel, A. R. Fersht, and S. P. Jackson.** 1999. The FHA domain is a modular phosphopeptide recognition motif. Mol. Cell **4:**387–394.
14. **Egyhazi, E., A. Ossoinak, O. Filhol-Cochet, C. Cochet, and A. Pigon.** 1999. The binding of the alpha subunit of protein kinase CK2 and RAP74 subunit of TFIIF to protein-coding genes in living cells is DRB sensitive. Mol. Cell. Biochem. **191:**149–159.
15. **Hilfiker, A., D. Hilfiker-Kleiner, A. Pannuti, and J. C. Lucchesi.** 1997. mof, a putative acetyl transferase gene related to the Tip60 and MOZ human genes and to the SAS genes of yeast, is required for dosage compensation in Drosophila. EMBO J. **16:**2054–2060.
16. **Hirohashi, Y., Q. Wang, Q. Liu, X. Du, H. Zhang, N. Sato, and M. I. Greene.** 2006. p78/MCRS1 forms a complex with centrosomal protein NdeI and is essential for cell viability. Oncogene **25:**4937–4946.
17. **Hofmann, K., and P. Bucher.** 1995. The FHA domain: a putative nuclear signalling domain found in protein kinases and transcription factors. Trends Biochem. Sci. **20:**347–349.
18. **Johnston, L. A.** 2009. Competitive interactions between cells: death, growth, and geography. Science **324:**1679–1682.
19. **Kind, J., J. M. Vaquerizas, P. Gebhardt, M. Gentzel, N. M. Luscombe, P. Bertone, and A. Akhtar.** 2008. Genome-wide analysis reveals MOF as a key regulator of dosage compensation and gene expression in Drosophila. Cell **133:**813–828.
20. **Komarnitsky, P., E. J. Cho, and S. Buratowski.** 2000. Different phosphorylated forms of RNA polymerase II and associated mRNA processing factors during transcription. Genes Dev. **14:**2452–2460.
21. **Lebedeva, L. A., E. N. Nabirochkina, M. M. Kurshakova, F. Robert, A. N. Krasnov, M. B. Evgen'ev, J. T. Kadonaga, S. G. Georgieva, and L. Tora.** 2005. Occupancy of the Drosophila hsp70 promoter by a subset of basal transcription factors diminishes upon transcriptional activation. Proc. Natl. Acad. Sci. U. S. A. **102:**18087–18092.
22. **Lee, J. M., and A. L. Greenleaf.** 1997. Modulation of RNA polymerase II elongation efficiency by C-terminal heptapeptide repeat domain kinase I. J. Biol. Chem. **272:**10990–10993.
23. **Lee, T. I., and R. A. Young.** 2000. Transcription of eukaryotic protein-coding genes. Annu. Rev. Genet. **34:**77–137.
24. **Li, J., G. I. Lee, S. R. Van Doren, and J. C. Walker.** 2000. The FHA domain mediates phosphoprotein interactions. J. Cell Sci. **113**(Pt. 23)**:**4143–4149.
25. **Li, X., L. Wu, C. A. S. Corsa, S. Kunkel, and Y. Dou.** 2009. Two mammalian MOF complexes regulate transcription activation by distinct mechanisms. Mol. Cell **36:**290–301.
26. **Li, Y., D. M. Keller, J. D. Scott, and H. Lu.** 2005. CK2 phosphorylates SSRP1 and inhibits its DNA-binding activity. J. Biol. Chem. **280:**11869–11875.
27. **Lin, D. Y., and H. M. Shih.** 2002. Essential role of the 58-kDa microspherule protein in the modulation of Daxx-dependent transcriptional repression as revealed by nucleolar sequestration. J. Biol. Chem. **277:**25446–25456.
28. **Marshall, N. F., J. Peng, Z. Xie, and D. H. Price.** 1996. Control of RNA polymerase II elongation potential by a novel carboxyl-terminal domain kinase. J. Biol. Chem. **271:**27176–27183.
29. **Marygold, S. J., J. Roote, G. Reuter, A. Lambertsson, M. Ashburner, G. H. Millburn, P. M. Harrison, Z. Yu, N. Kenmochi, T. C. Kaufman, S. J. Leevers, and K. R. Cook.** 2007. The ribosomal protein genes and Minute loci of Drosophila melanogaster. Genome Biol. **8:**R216.
30. **Mendjan, S., M. Taipale, J. Kind, H. Holz, P. Gebhardt, M. Schelder, M. Vermeulen, A. Buscaino, K. Duncan, J. Mueller, M. Wilm, H. G. Stunnenberg, H. Saumweber, and A. Akhtar.** 2006. Nuclear pore components are involved in the transcriptional regulation of dosage compensation in Drosophila. Mol. Cell **21:**811–823.
31. **Nybakken, K., S. A. Vokes, T. Y. Lin, A. P. McMahon, and N. Perrimon.** 2005. A genome-wide RNA interference screen in Drosophila melanogaster cells for new components of the Hh signaling pathway. Nat. Genet. **37:**1323–1332.
32. **Orphanides, G., T. Lagrange, and D. Reinberg.** 1996. The general transcription factors of RNA polymerase II. Genes Dev. **10:**2657–2683.
33. **Payne, J. M., P. J. Laybourn, and M. E. Dahmus.** 1989. The transition of RNA polymerase II from initiation to elongation is associated with phosphorylation of the carboxyl-terminal domain of subunit IIa. J. Biol. Chem. **264:**19621–19629.
34. **Prestel, M., C. Feller, T. Straub, H. Mitlöhner, and P. B. Becker.** 2010. The activation potential of MOF is constrained for dosage compensation. Mol. Cell **38:**815–826.
35. **Raja, S. J., I. Charapitsa, T. Conrad, J. M. Vaquerizas, P. Gebhardt, H. Holz, J. Kadlec, S. Fraterman, N. M. Luscombe, and A. Akhtar.** 2010. The nonspecific lethal complex is a transcriptional regulator in Drosophila. Mol. Cell **38:**827–841.
36. **Rea, S., G. Xouri, and A. Akhtar.** 2007. Males absent on the first (MOF): from flies to humans. Oncogene **26:**5385–5394.
37. **Roberts, S. G., B. Choy, S. S. Walker, Y. S. Lin, and M. R. Green.** 1995. A role for activator-mediated TFIIB recruitment in diverse aspects of transcriptional regulation. Curr. Biol. **5:**508–516.
38. **Roeder, R. G.** 1996. The role of general initiation factors in transcription by RNA polymerase II. Trends Biochem. Sci. **21:**327–335.
39. **Rubin, G. M., and A. C. Spradling.** 1982. Genetic transformation of Drosophila with transposable element vectors. Science **218:**348–353.
40. **Sauer, K., K. Weigmann, S. Sigrist, and C. F. Lehner.** 1996. Novel members of the cdc2-related kinase family in Drosophila: cdk4/6, cdk5, PFTAIRE, and PITSLRE kinase. Mol. Biol. Cell **7:**1759–1769.
41. **Saunders, A., L. J. Core, and J. T. Lis.** 2006. Breaking barriers to transcription elongation. Nat. Rev. Mol. Cell Biol. **7:**557–567.
42. **Schroeder, S. C., B. Schwer, S. Shuman, and D. Bentley.** 2000. Dynamic association of capping enzymes with transcribing RNA polymerase II. Genes Dev. **14:**2435–2440.
43. **Shimono, K., Y. Shimono, K. Shimokata, N. Ishiguro, and M. Takahashi.** 2005. Microspherule protein 1, Mi-2beta, and RET finger protein associate in the nucleolus and up-regulate ribosomal gene transcription. J. Biol. Chem. **280:**39436–39447.
44. **Shogren-Knaak, M., H. Ishii, J. M. Sun, M. J. Pazin, J. R. Davie, and C. L. Peterson.** 2006. Histone H4-K16 acetylation controls chromatin structure and protein interactions. Science **311:**844–847.
45. **Smith, E. R., A. Pannuti, W. Gu, A. Steurnagel, R. G. Cook, C. D. Allis, and J. C. Lucchesi.** 2000. The *Drosophila* MSL complex acetylates histone H4 at lysine 16, a chromatin modification linked to dosage compensation. Mol. Cell. Biol. **20:**312–318.
46. **Taipale, M., S. Rea, K. Richter, A. Vilar, P. Lichter, A. Imhof, and A. Akhtar.** 2005. hMOF histone acetyltransferase is required for histone H4 lysine 16 acetylation in mammalian cells. Mol. Cell. Biol. **25:**6798–6810.
47. **Trembley, J. H., D. Hu, L. C. Hsu, C. Y. Yeung, C. Slaughter, J. M. Lahti, and V. J. Kidd.** 2002. PITSLRE p110 protein kinases associate with transcription complexes and affect their activity. J. Biol. Chem. **277:**2589–2596.
48. **Trembley, J. H., D. Hu, C. A. Slaughter, J. M. Lahti, and V. J. Kidd.** 2003. Casein kinase 2 interacts with cyclin-dependent kinase 11 (CDK11) in vivo and phosphorylates both the RNA polymerase II carboxyl-terminal domain and CDK11 in vitro. J. Biol. Chem. **278:**2265–2270.

49. **Weeks, J. R., D. E. Coulter, and A. L. Greenleaf.** 1982. Immunological studies of RNA polymerase II using antibodies to subunits of Drosophila and wheat germ enzyme. J. Biol. Chem. **257:**5884–5892.
50. **Wu, J. L., Y. S. Lin, C. C. Yang, Y. J. Lin, S. F. Wu, Y. T. Lin, and C. F. Huang.** 2009. MCRS2 represses the transactivation activities of Nrf1. BMC Cell Biol. **10:**9.
51. **Xu, T., and G. M. Rubin.** 1993. Analysis of genetic mosaics in developing and adult Drosophila tissues. Development **117:**1223–1237.
52. **Yang, L., N. Li, C. Wang, Y. Yu, L. Yuan, M. Zhang, and X. Cao.** 2004. Cyclin L2, a novel RNA polymerase II-associated cyclin, is involved in pre-mRNA splicing and induces apoptosis of human hepatocellular carcinoma cells. J. Biol. Chem. **279:**11639–11648.
53. Reference deleted.
54. **Zawel, L., K. P. Kumar, and D. Reinberg.** 1995. Recycling of the general transcription factors during RNA polymerase II transcription. Genes Dev. **9:**1479–1490.